Critical behavior in ultrastrong-coupled oscillators

Vivishek Sudhir,[1,*] Marco G. Genoni,[1] Jinhyoung Lee,[2] and M. S. Kim[1]

[1]*QOLS, Blackett Laboratory, Imperial College London, London SW7 2BW, United Kingdom*

[2]*Physics Department, Hanyang University, Sungdong-Gu, Seoul KR-133-791, South Korea*

(Received 3 April 2012; published 16 July 2012)

We investigate the strong-coupling regime of a linear x-x coupled harmonic-oscillator system by performing a direct diagonalization of the Hamiltonian. It is shown that the x-x coupled Hamiltonian can be equivalently described by a Mach-Zehnder-type interferometer with a quadratic unitary operation in each of its arms. We show a sharp transition of the unitary operation from an elliptical phase rotator to an elliptical squeezer as the coupling gets stronger, leading to the continuous generation of entanglement, even for a significantly thermal state in the ultrastrong-coupled regime. It is also shown that this critical regime cannot be achieved by a classical Hookian coupling. Finally, the effect of a finite-temperature environment is analyzed, showing that entanglement can still be generated from a thermal state in the ultrastrong-coupled regime but is destroyed rapidly.

DOI: 10.1103/PhysRevA.86.012316 PACS number(s): 03.67.Bg, 42.50.Ct, 42.50.St

I. INTRODUCTION

Strong coupling, which is one of the key ingredients for the manipulation and control of quantum systems, makes quantum-mechanical predictions distinct from classical ones. In fact, the definition of strong coupling in quantum mechanics has evolved over the years. In atomic and optical physics, strong coupling was defined to show Autler-Townes splitting [1] in which the atom-field interaction is stronger than the atomic-decay rate. The next age of strong coupling was defined in cavity quantum electrodynamics (QED) where an atom-field interaction strong in comparison to the cavity and atomic-decay rates can be realized. A series of important experiments have been performed to show the nonclassical nature of the atom-field interaction for Rydberg atoms in microwave cavities [2,3]. This regime was recently also attained with a cavity optomechanical system [4]. But with a system consisting of superconducting Josephson junctions coupled to microwave fields in stripline resonators, the interaction strength can be made even stronger than the atom-field coupling realized previously in cavity QED [5,6]. These so-called circuit-QED systems can reach coupling strengths comparable to the transition frequency of the relevant qubit system. In these systems, we find interesting phenomena such as the breakdown of the rotating-wave approximation and the emergence of a unique deep strong-coupling regime [7].

A system of coupled oscillators has been of interest in various contexts as several physical systems are represented by harmonic oscillators, such as nanomechanical oscillators, electromagnetic fields, and many two-level systems. Hopfield studied the quantization of an electromagnetic field in a dispersive medium using a coupled harmonic oscillator model [8]. Recently, such a system of coupled oscillators has been considered as a possible mechanism to generate entanglement in an array of nanoelectromechanical devices [9–11]. In this paper, we study ultrastrong coupling between harmonic oscillators where the coupling rate g is comparable to or larger than the natural frequencies ω_j of the harmonic oscillators. Strongly coupled oscillators in which the counter-rotating terms are not negligible have been studied in the context of twin-photon generation [12]. The study of such systems is supported by recent experimental progress wherein such a regime is becoming accessible, for instance in the interaction of multiple quantum wells with terahertz electromagnetic fields [13]. In this paper, we go even further than the strong-coupling regime and find a critical point in the coupling strength at which the evolution of the oscillator states radically changes. An equivalent regime was studied for the interaction between an atom and a field [7,14] where photon-number wave packets were found to experience collapse and revivals across parity chains in Hilbert space. The model that we consider here is quite different in the sense that we have a bosonic system living in an infinite dimensional Hilbert space so that there is no such parity-defined dynamics. However, the model is exactly solvable, and we find critical effects from the dynamics of the coupled oscillators, which manifests in the entanglement behavior.

We consider a system of two bosonic oscillators interacting via a quadratic interaction, whose Hamiltonian is described by

$$\hat{H} = \sum_{j=1}^{2} \frac{\omega_j}{2}\left(\hat{p}_j^2 + \hat{x}_j^2\right) + g\hat{x}_1\hat{x}_2, \tag{1}$$

where the dimensionless quadrature operators satisfy the canonical commutation relation, i.e., $[\hat{x}_j,\hat{p}_k] = i\delta_{jk}$. For instance, the Dicke model of superradiance [15] is approximately described by such a Hamiltonian. In the context of cavity optomechanical systems, such a linearized Hamiltonian describes the dynamics when the mechanics is being driven by a strong coherent field [16]. In fact, this linearized model has been investigated previously in the optomechanics context [17] in the rotating-wave approximation (RWA), which is possible when the system is relatively weakly coupled.

In this paper, we will show that in the ultrastrong-coupling regime, the non-RWA terms turn out to be not only important but also to critically change the oscillator interaction. After identifying a unitary transformation exactly diagonalizing the Hamiltonian of Eq. (1), we show its equivalence to a Mach-Zehnder-type setup with unitary operations in its arms, thereby explaining the generation of entanglement in the model. At

[*]Current address: LPQM, École Polytechnique Fédérale de Lausanne (EPFL), 1015 Lausanne, Switzerland.

the critical point when the coupling becomes ultrastrong, we observe the transition of the unitary operation from an elliptic rotator to a squeezer. This transition is clearly reflected in the entanglement dynamics of the oscillators. It is interesting to note that the classical Hookian model for classical harmonic oscillators is not able to reach this critical point.

II. DIAGONALIZATION OF THE HAMILTONIAN

One can codify the operator Hamiltonian (1) in terms of a Hamiltonian matrix

$$H = \begin{bmatrix} \omega_1 & g \\ g & \omega_2 \end{bmatrix} \oplus \begin{bmatrix} \omega_1 & 0 \\ 0 & \omega_2 \end{bmatrix} \equiv H_x \oplus H_p \tag{2}$$

expressed in the basis defined by the column vector of quadratures $\hat{R} = (\hat{x}_1, \hat{x}_2, \hat{p}_1, \hat{p}_2)^{\mathsf{T}}$ so that $\hat{H} = \frac{1}{2}\hat{R}^{\mathsf{T}} H \hat{R}$, where we also define the diagonal block matrices corresponding to positions and momenta.

The usual diagonalization of such a quadratic Hamiltonian proceeds by defining normal-mode operators $\hat{\Omega}_q$ ($q = \pm$) and their Hermitian conjugates, which are linear combinations of the bare quadratures satisfying $[\hat{\Omega}_q, \hat{H}] = E_q \hat{\Omega}_q$. Specifically, the normal-mode energies are found to be $E_\pm^2 = \omega_1^2 + \omega_2^2 \pm \sqrt{(\omega_1^2 + \omega_2^2)^2 + 4\omega_1\omega_2(g^2 - \omega_1\omega_2)}$ from which we already observe an interesting regime where E_- is imaginary for $g > g_c \equiv \sqrt{\omega_1\omega_2}$.

The transformation to normal modes is just a symplectomorphism [18]. The Hamiltonian matrix can be diagonalized by a symplectic matrix $S \in Sp(4,\mathbb{R})$ such that it is block diagonal of the form $S = S_x \oplus S_p$. The diagonal Hamiltonian matrix is then $H' = S^{\mathsf{T}} H S = (S_x^{\mathsf{T}} H_x S_x) \oplus (S_p^{\mathsf{T}} H_p S_p)$. From the general conditions to be satisfied by symplectic transformations, we get that for $S_x, S_p \in SL(2,\mathbb{R})$, $S_p^{\mathsf{T}} = S_x^{-1}$. The unitary representation of S in the Hilbert space of the system is

$$\hat{T} = \exp[i(A\hat{x}_1\hat{p}_2 - B\hat{x}_2\hat{p}_1)], \tag{3}$$

parametrized by real constants A and B. This diagonalizes $\hat{H}$ to $\hat{H}' = \hat{T}\hat{H}\hat{T}^\dagger$ if and only if

$$\tan 2\sqrt{AB} = \frac{2gg_c}{\omega_1^2 - \omega_2^2}, \quad \frac{A}{B} = \frac{\omega_2}{\omega_1}. \tag{4}$$

The diagonal Hamiltonian is then given by

$$\hat{H}' = \omega_1 \hat{p}_1^2 + \left(\frac{\omega_1}{2}c^2 + \frac{\omega_2^2}{2\omega_1}s^2 + \frac{gg_c}{\omega_1}cs\right)\hat{x}_1^2 + \omega_2\hat{p}_2^2 + \left(\frac{\omega_2}{2}c^2 + \frac{\omega_1^2}{2\omega_2}s^2 - \frac{gg_c}{\omega_2}cs\right)\hat{x}_2^2, \tag{5}$$

where we denote $c = \cos\sqrt{AB}$ and $s = \sin\sqrt{AB}$. Each normal mode is described by a quadratic Hamiltonian, which looks very similar to a standard free Hamiltonian for an oscillator. But using the condition (4), it is found that the last term in Eq. (5) is zero (negative) when $g = g_c$ ($g > g_c$) so that these are standard harmonic oscillators only when $g < g_c$. The first (second) mode in Eq. (5) is associated with E_+ (E_-), which we call the "+" ("−") mode. When $g = g_c$, the "−" mode does not have a bound spectrum but is rather a free particle while the "+" mode is still a harmonic oscillator. Increasing the coupling strength further, for $g > g_c$, the anomalous "−" mode is dynamically unstable since it is driven by a force derived from the inverted harmonic potential. So, the earlier observation of E_- becoming imaginary is reflected by this qualitative change in the dynamical behavior of the system as the coupling strength crosses its critical value g_c.

III. INEQUIVALENCE TO CLASSICAL COUPLED OSCILLATORS

An obvious intuition one would have from thinking about the classical oscillating systems is that the model (1) must be the quantized version of the classical Hookian Hamiltonian for coupled oscillators,

$$\hat{H}_C = \sum_{j=1}^{2}\left(\frac{\hat{P}_j^2}{2m} + \frac{1}{2}m\omega^2\hat{X}_j^2\right) + \frac{m\mathcal{G}^2}{2}(\hat{X}_1 - \hat{X}_2)^2, \tag{6}$$

where m is the common mass of the particle, ω the common natural frequency, and $\mathcal{G}$ the Hookian coupling rate. The oscillators are assumed to be identical for simplicity (a generalization is straightforward). Introducing dimensionless quadratures $\hat{x}_{1,2} = (m\omega_0)^{1/2}\hat{X}_{1,2}$ and $\hat{p}_{1,2} = (m\omega_0)^{-1/2}\hat{P}_{1,2}$ with the renormalized frequency $\omega_0 = \sqrt{\omega^2 + \mathcal{G}^2}$, the Hamiltonian becomes

$$\hat{H}_C = \frac{\omega_0}{2}\left[\left(\hat{p}_1^2 + \hat{x}_1^2\right) + \left(\hat{p}_2^2 + \hat{x}_2^2\right) - G\hat{x}_1\hat{x}_2\right],$$

where $G = \frac{\mathcal{G}^2}{\omega^2 + \mathcal{G}^2}$ is the renormalized coupling strength. So, it is clear that in the quantum version of the classical Hookian problem, the ultrastrong-coupling regime (here, $G > 1$) is not possible to achieve.

The ultrastrong-coupling transition of the form exhibited by the Hamiltonian (1) seems to be a property of such quantum-coupling models and not something that is seen easily in the standard harmonic-oscillator model. In particular though, for optomechanical problems, the linearization of the actual radiation-pressure interaction $(\hat{p}_1^2 + \hat{x}_1^2)\hat{x}_2$ (which leads to $\hat{x}_1\hat{x}_2$) is valid only for a short interaction time. Otherwise, the displacement of the mechanics gets too large, and the approximation leading to the interaction Hamiltonian breaks down in the strong-coupling regime $g > g_c$ [19–21].

IV. ENTANGLEMENT DYNAMICS

In the resonant case, i.e., $\omega_1 = \omega_2$ and so $A = B = \frac{\pi}{4}$, the transformation operator $\hat{T}$ in Eq. (3) becomes exactly the same as the 50:50 beam-splitter operator. Thus, the evolution operator $\hat{\mathcal{U}}(t) = e^{-i\hat{H}t}$ corresponding to the Hamiltonian (1) can be factorized into $\hat{\mathcal{U}}(t) = \hat{T}^\dagger e^{-i\hat{H}'_- t} e^{-i\hat{H}'_+ t}\hat{T}$, where $\hat{H}'_\pm = \frac{1}{2}[\omega_{1,2}\hat{p}_{1,2}^2 + (g_c \pm g)\hat{x}_{1,2}^2]$. It is now obvious that in the resonant case, the dynamics is equivalently represented by a Mach-Zehnder interferometer with 50:50 beam splitters as shown in Fig. 1 but with some active operations in both arms [22].

To determine the kind of active operations, consider the individual evolutions generated by $\hat{H}_\pm$ which are of the quadratic form, $\hat{H}_q = \frac{1}{2}(\alpha_q^2\hat{x}_q^2 + \beta_q^2\hat{p}_q^2)$ ($q = \pm$). The evolution of the

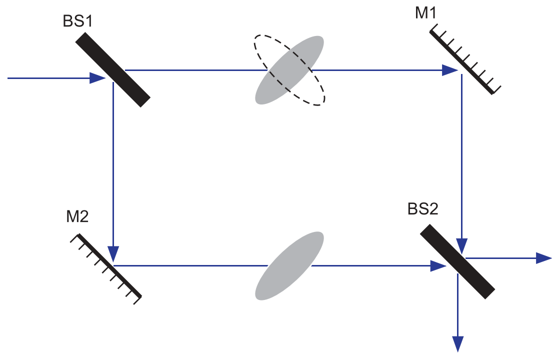

FIG. 1. (Color online) The evolution due to Hamiltonian (1) is equivalent to a Mach-Zehnder setup for the resonant case such that one arm of the interferometer experiences elliptic rotation and the other arm undergoes elliptic rotation (squeezing) if $g < g_c$ ($g > g_c$). BS: Beam splitter, M: Mirror.

quadrature operators induced by such a Hamiltonian is

$$\begin{pmatrix} \hat{x}_q(t) \\ \hat{p}_q(t) \end{pmatrix} = \begin{pmatrix} \cos\alpha_q\beta_q t & -\frac{\beta_q}{\alpha_q}\sin\alpha_q\beta_q t \\ \frac{\alpha_q}{\beta_q}\sin\alpha_q\beta_q t & \cos\alpha_q\beta_q t \end{pmatrix} \begin{pmatrix} \hat{x}_q(0) \\ \hat{p}_q(0) \end{pmatrix}.$$

The transformation shows the behavior of an elliptical rotator where the product of the quadrature scaling factors is unity. It preserves the quadrature uncertainties, leading to, at most, squeezing of the mode. Importantly, if either α_q or β_q is negative, the elliptical rotator becomes an elliptical squeezer; this is precisely the situation for the "$-$" mode when the coupling is ultrastrong, i.e., $g > g_c$. It is also worth noting that in the general nonresonant case, both the beam-splitting and two-mode squeezing terms appear in $\hat{T}$, meaning that instead of the passive beam splitters at the entry and exit ports, one will have another active device in the equivalent picture.

From the equivalent Mach-Zehnder picture, the source of entanglement is obvious: squeezing in the input fields is a necessary condition for Gaussian-entangled output from a beam splitter [23]. The interaction leads to significantly more entanglement when $g = g_c$ than the case for which $g < g_c$. To explicitly study dynamic entanglement, we consider each harmonic oscillator initially in its thermal equilibrium so that the total density operator $\hat{\rho}(0) = \hat{\rho}_1^{\mathrm{Th}} \otimes \hat{\rho}_2^{\mathrm{Th}}$, where $\hat{\rho}_j^{\mathrm{Th}} = \frac{1}{\mathcal{Z}_j}\exp[-\frac{\delta_j}{2}(\hat{x}_j^2 + \hat{p}_j^2)]$ with the canonical partition function $\mathcal{Z}_j$ and mean excitation number $\eta_j = (e^{\delta_j} - 1)^{-1}$. $\delta_j = \omega_j / k_B T_j$ at temperature T_j with the Boltzmann constant k_B.

Figure 2(a) shows the dynamic entanglement, measured by the logarithmic negativity [24,25], for a thermal state with a single average excitation (see Appendix A for explicit formulas of the log negativity). We observe that for $g < g_c$, the entanglement has an oscillatory behavior with typical periods related to the frequencies of the normal modes. When $g = g_c$, the entanglement monotonically increases, disregarding the small oscillations due to the "+" normal mode. The same behavior is observed for larger values of the coupling constant ($g > g_c$) in Fig. 2(b) where we plot the "seralian" Δ [26] which, in the unitary case, is a sufficient entanglement monotone (see Appendix A for details). The entanglement keeps increasing with time (neglecting the small oscillations), and in particular at a fixed time, the larger the value of the

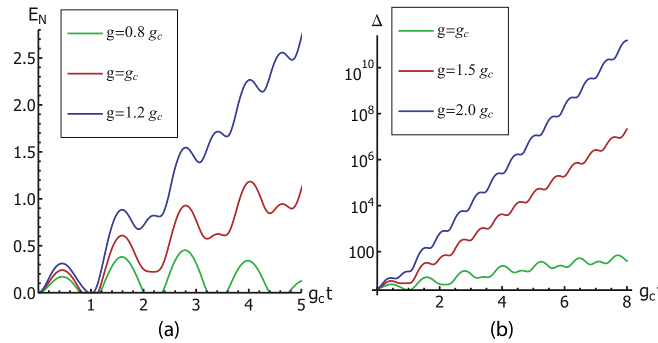

FIG. 2. (Color online) (a) Log negativity and (b) the seralian for the thermal state with $\eta_1 = 0, \eta_2 = 1$ for various coupling strengths at $\omega_1 = 5\omega_2$.

coupling constant g, the larger is the entanglement achieved. This particular behavior can be explained also by looking at the eigenvalues of the Hamiltonian matrix H. For $g < g_c$, the matrix is positive definite, and as proved in Ref. [27], the corresponding unitary operator will recur to the identity for a given time. For larger values of g, the matrix H is not positive definite anymore, the recurrence property of the evolution is lost, and the entanglement increases with time.

Even when the initial state is significantly thermal, if the system is critically coupled, entanglement can be generated as depicted in Fig. 3. In fact, we also observe that the purity of one oscillator is an important factor in the generation of entanglement. When one oscillator is pure, the maximum degree of entanglement achieved remains about the same regardless of the temperature of the other oscillator. The importance of single-system purity was also observed in some other interaction models [28,29].

A. Dissipative dynamics

Let us consider now the case in which the system interacts with a noisy environment. Because of the environment interaction, we observe that the supercritical regime $g > g_c$ can cease to be dynamically unstable. Assuming that each bare oscillator interacts with its respective thermal environment with mean excitation $\bar{n}_j$, under the Born-Markov approximation, the evolution of the system density matrix is governed by the

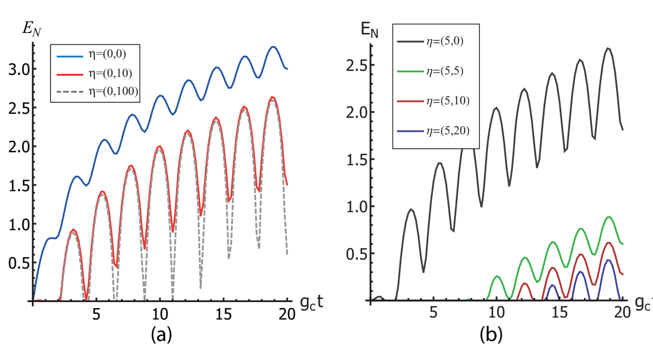

FIG. 3. (Color online) Dynamic entanglement at $g = g_c$ for increasing the degree of thermality when one oscillator is initially (a) in a pure state ($\eta_1 = 0$) and (b) in a thermally excited state ($\eta_1 = 5$). The two oscillators are resonant.

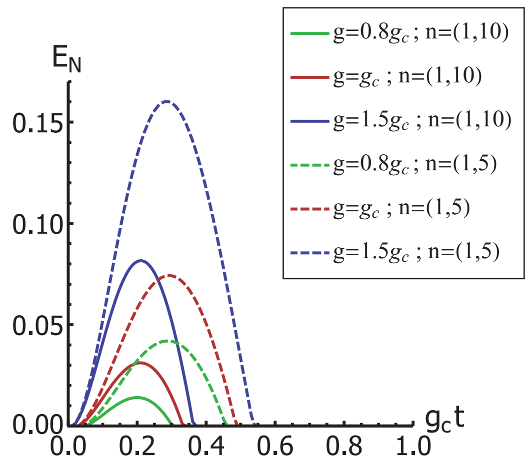

FIG. 4. (Color online) Dynamic entanglement for the dissipative case for each of the three regimes. Here the oscillator 1 (2) is coupled to an environment of $\bar{n}_1 = 1$ at a rate $\gamma_1 = 0.01\omega_1$ ($\gamma_2 = 0.25\omega_2$).

Kossakowski-Lindblad master equation

$$\frac{d\hat{\rho}}{dt} = -i[\hat{H},\hat{\rho}] + \sum_{j=1}^{2} \frac{\gamma_j}{2}\{(\bar{n}_j + 1)\mathcal{L}[\hat{a}_j] + \bar{n}_j \mathcal{L}[\hat{a}_j^\dagger]\}\hat{\rho}, \qquad (7)$$

where $\mathcal{L}[\hat{O}]\hat{\rho} = 2\hat{O}\hat{\rho}\hat{O}^\dagger - \hat{O}^\dagger\hat{O}\hat{\rho} - \hat{\rho}\hat{O}^\dagger\hat{O}$ is the Liouvillian while γ_j is the rate at which the jth mode is coupled to the environment [see Appendix B for the analytical solution of Eq. (7)].

The logarithmic negativity E_N can be evaluated, and the results are plotted in Fig. 4 for various values of the coupling strength. We observe that, as expected, also in the supercritical regime $g > g_c$, the entanglement reaches a maximum value and then starts to decrease and eventually reaches zero for a given time t_0. Not surprisingly, larger values of the coupling constant and lower values of the noisy parameters η_j, γ_j, and $\bar{n}_j$ correspond to larger maximum values of entanglement and to larger values of the zero-entanglement time t_0.

V. CONCLUSION

We have investigated the ultrastrong-coupled regime of a linear x-x coupled quantum harmonic oscillator system. Three different regimes of qualitatively different dynamical behavior can be identified from the normal modes of the system. In particular, in the supercritical regime $g > g_c$, the "$-$" mode has an anomalous accelerating motion, which can be understood as a consequence of a lack of translation symmetry in the Hamiltonian (1) so that momentum conservation is not explicitly guaranteed. In the classical Hookian Hamiltonian (6), such a symmetry is manifest so that no dynamical anomaly is allowed in the strong-coupling regime.

We further find that these three regimes, characterized by their dynamical behaviors, are also uniquely characterized by the dynamics of entanglement; in particular, the supercritical regime is one where entanglement can be unboundedly generated from even a highly thermal state. A similar behavior was studied in the context of the superradiant phase transition of the Dicke model, whose effective Hamiltonian is of the form of Eq. (1) after a Holstein-Primakoff transformation of a set of SU(2) operators into a bosonic operator.

Finally, we also note that the supercritical regime exhibits a finite entanglement even though the system may be coupled to a decohering Markovian environment at a nonzero temperature.

ACKNOWLEDGMENTS

M.S.K. thanks Wonmin Son for discussions. This work was supported by the Qatar National Research Fund (NPRP Grant No. 4-554-1-084). J.L. acknowledges support from a National Research Foundation of Korea (NRF) Grant (No. 2010-0015059). M.G.G. acknowledges fellowship support from UK EPSRC (No. EP/I026436/1) and thanks Alessio Serafini and Matteo Binazzi for interesting and useful discussions.

APPENDIX A: LOG NEGATIVITY FOR GAUSSIAN STATES

Given a two-mode Gaussian state, its entanglement properties are fully characterized by its covariance matrix $\boldsymbol{\sigma}$, which can be written in terms of 2×2 matrices as

$$\boldsymbol{\sigma} = \begin{pmatrix} \boldsymbol{\sigma}_1 & \boldsymbol{\gamma} \\ \boldsymbol{\gamma}^\mathsf{T} & \boldsymbol{\sigma}_2 \end{pmatrix}. \qquad (A1)$$

The log negativity [24] of the two-mode state can be evaluated as $E_N(\varrho) = \max[0, -\log_e(2\tilde{\nu}_-)]$, where $\tilde{\nu}_-$ is the lowest symplectic eigenvalue of the corresponding partial transposed state. In the formula we have

$$\tilde{\nu}_-^2 = \frac{\Delta - \sqrt{\Delta^2 - 4\mathrm{Det}[\boldsymbol{\sigma}]}}{2}, \qquad (A2)$$

where the seralian Δ is defined as

$$\Delta = \mathrm{Det}[\boldsymbol{\sigma}_1] + \mathrm{Det}[\boldsymbol{\sigma}_2] - 2\mathrm{Det}[\boldsymbol{\gamma}] \qquad (A3)$$

and where $\mathrm{Det}[A]$ denotes the determinant of the matrix A. It is known that the logarithmic negativity E_N is an entanglement monotone [25]. One should also note that $\mathrm{Det}[\boldsymbol{\sigma}]$ is directly related to the purity of the state since $\mathrm{Tr}[\varrho^2] = 1/(2\sqrt{\mathrm{Det}[\boldsymbol{\sigma}]})$. As a consequence, unitary evolution leaves $\mathrm{Det}[\boldsymbol{\sigma}]$ invariant so that the log negativity is monotonous with Δ. For this reason, when we consider the entanglement dynamics due to nondissipative evolution, we may take the seralian Δ to be an entanglement monotone.

APPENDIX B: SOLVING THE MASTER EQUATION

The master equation (7) can be cast into a c-number partial differential equation (PDE) by introducing the symmetric ordered characteristic function $\chi(\alpha_1,\alpha_2;t) = \mathrm{Tr}[\hat{D}_1(\alpha_1)\hat{D}_2(\alpha_2)\hat{\rho}(t)]$, where $\hat{D}_j(\alpha_j) = \exp(\alpha_j\hat{a}_j^\dagger - \alpha_j^*\hat{a}_j)$. We choose to express the PDE in terms of the quadratures parameters x_j, p_j, defined via $\alpha_j = \frac{1}{\sqrt{2}}(x_j + i p_j)$, so that we get the Fokker-Planck equation

$$\frac{\partial \chi}{\partial t} = -\frac{1}{2}(\mathrm{r}^\mathsf{T}\bar{\Gamma}\mathrm{r})\chi + \frac{1}{2}\left[\mathrm{r}^\mathsf{T}\left(\Upsilon\widetilde{H} - \frac{1}{2}\Gamma\right)\overrightarrow{\partial_\mathrm{r}}\right]\chi + \frac{1}{2}\chi\left[\overleftarrow{\partial_\mathrm{r}^\mathsf{T}}\left((\Upsilon\widetilde{H})^\mathsf{T} - \frac{1}{2}\Gamma\right)\mathrm{r}\right], \qquad (B1)$$

where we define the vector $\mathsf{r} = (x_1, p_1, x_2, p_2)^\mathsf{T}$, the associated gradient operator $\partial_\mathsf{r} = (\partial_{x_1}, \partial_{p_1}, \partial_{x_2}, \partial_{p_2})^\mathsf{T}$, and the matrices

$$\Upsilon = \bigoplus_{j=1}^{2} \begin{bmatrix} 0 & 1 \\ -1 & 0 \end{bmatrix}, \quad \Gamma = \bigoplus_{j=1}^{2} \begin{bmatrix} \gamma_j & 0 \\ 0 & \gamma_j \end{bmatrix},$$

$$\bar{\Gamma} = \bigoplus_{j=1}^{2} \begin{bmatrix} \gamma_j \left(\bar{n}_j + \frac{1}{2}\right) & 0 \\ 0 & \gamma_j \left(\bar{n}_j + \frac{1}{2}\right) \end{bmatrix},$$

and where $\widetilde{H}$ here is a permutation on the Hamiltonian matrix (2) corresponding to the difference in the order chosen for the quadrature variables. The arrows on the gradient operators denote the direction in which the differential operators act.

As shown above, the system Hamiltonian only affects elliptic rotations or elliptic squeezing in the course of the dynamics so that an initial Gaussian state localized at the origin in phase space remains so always. And since the bath is in thermal equilibrium, it too does not affect any finite displacements in phase space but only scale and rotation changes. Thus, for our relevant case, without loss of generality, we choose the ansatz

$$\chi(\mathsf{r}; t) = \exp\left[-\frac{1}{2}\mathsf{r}^\mathsf{T}\sigma(t)\mathsf{r}\right],$$

where now the time dependence is carried in the covariance matrix. Substituting this into Eq. (B1) and then identifying the coefficients of the various bilinear products, we get the equation of motion for the covariance matrix, viz.,

$$\frac{d\sigma}{dt} + \left(\frac{1}{2}\Gamma - \Upsilon\widetilde{H}\right)\sigma + \sigma\left(\frac{1}{2}\Gamma - \Upsilon\widetilde{H}\right)^\mathsf{T} = \bar{\Gamma}.$$

This has the solution

$$\sigma(t) = K(t)\left\{\sigma(0) + \int_0^t K(-\tau)\bar{\Gamma}K^\mathsf{T}(-\tau)d\tau\right\}K^\mathsf{T}(t),$$

where $K(t) = \exp[(\Upsilon\widetilde{H} - \frac{1}{2}\Gamma)t]$.

[1] S. Autler and C. Townes, Phys. Rev. **100**, 703 (1955).
[2] J. M. Raimond, M. Brune, and S. Haroche, Rev. Mod. Phys. **73**, 565 (2001).
[3] S. Haroche and J. M. Raimond, *Exploring the Quantum* (Oxford University Press, Oxford, 2006).
[4] E. Verhagen, S. Deleglise, S. Weis, A. Schliesser, and T. J. Kippenberg, Nature (London) **482**, 63 (2012).
[5] A. Wallraff, D. I. Schuster, A. Blais, L. Frunzio, R. S. Huang, J. Majer, S. Kumar, S. M. Girvin, and R. J. Schoelkopf, Nature (London) **431**, 162 (2004).
[6] T. Niemczyk, F. Deppe, H. Huebl, E. Menzel, F. Hocke, M. Schwarz, J. Garcia-Ripoo, D. Zueco, T. Hümmer, E. Solano *et al.*, Nat. Phys. **6**, 772 (2010).
[7] J. Casanova, G. Romero, I. Lizuain, J. J. Garcia-Ripoll, and E. Solano, Phys. Rev. Lett. **105**, 263603 (2010).
[8] J. J. Hopfield, Phys. Rev. **112**, 1555 (1958).
[9] J. Eisert, M. B. Plenio, S. Bose, and J. Hartley, Phys. Rev. Lett. **93**, 190402 (2004).
[10] K. Audenaert, J. Eisert, M. B. Plenio, and R. F. Werner, Phys. Rev. A **66**, 042327 (2002).
[11] F. Galve, L. A. Pachon, and D. Zueco, Phys. Rev. Lett. **105**, 180501 (2010).
[12] C. Ciuti, G. Bastard, and I. Carusotto, Phys. Rev. B **72**, 115303 (2005).
[13] G. Günter, A. A. Anappara, J. Hees, A. Sell, G. Biasiol, L. Sorba, S. D. Liberato, C. Ciuti, A. Tredicucci, A. Leitenstorfer *et al.*, Nature (London) **458**, 178 (2009).
[14] M. Bina, G. Romero, J. Casanova, J. J. Garcia-Ripoll, A. Lulli, F. Casagrande, and E. Solano, Eur. Phys. J. **203**, 207 (2012).
[15] R. H. Dicke, Phys. Rev. **93**, 99 (1968).
[16] S. Mancini and P. Tombesi, Phys. Rev. A **49**, 4055 (1994).
[17] U. Akram, N. Kiesel, M. Aspelmeyer, and G. J. Milburn, New J. Phys. **12**, 083030 (2010).
[18] D. McDuff and D. Salamon, *Introduction to Symplectic Topology* (Oxford University Press, Oxford, 1998).
[19] C. K. Law, Phys. Rev. A **51**, 2537 (1995).
[20] A. F. Pace, M. J. Collett, and D. F. Walls, Phys. Rev. A **47**, 3173 (1993).
[21] M. R. Vanner, I. Pikovski, G. D. Cole, M. S. Kim, C. Brukner, K. Hammerer, G. J. Milburn, and M. Aspelmeyer, Proc. Natl. Acad. Sci. USA **108**, 16182 (2011).
[22] M. Paternostro, M. S. Kim, E. Park, and J. Lee, Phys. Rev. A **72**, 052307 (2005).
[23] M. S. Kim, W. Son, V. Bužek, and P. L. Knight, Phys. Rev. A **65**, 032323 (2002).
[24] G. Vidal and R. F. Werner, Phys. Rev. A **65**, 032314 (2002); J. Lee, M. S. Kim, Y. J. Park, and S. Lee, J. Mod. Opt. **47**, 2151 (2000).
[25] M. B. Plenio, Phys. Rev. Lett. **95**, 090503 (2005).
[26] A. Serafini, F. Illuminati, and S. De Siena, J. Phys. B **37**, L21 (2004).
[27] M. G. Genoni, A. Serafini, M. S. Kim, and D. Burgarth, Phys. Rev. Lett. **108**, 150501 (2012).
[28] S. Bose, I. Fuentes-Guridi, P. L. Knight, and V. Vedral, Phys. Rev. Lett. **87**, 050401 (2001).
[29] M. S. Kim, J. Lee, D. Ahn, and P. L. Knight, Phys. Rev. A **65**, 040101(R) (2002).